

# AN EVOLUTIONARY GAME THEORY APPROACH TO MODELING BEHAVIOURAL INTERACTION IN DISCLOSING INFECTION BEGINS WITH AN OUTBREAK: COVID-19 AS AN EXAMPLE

PRANAV VERMA, VINEY KUMAR, SAMIT BHATTACHARYYA

**ABSTRACT.** The global impact of the COVID-19 pandemic on the livelihoods of people worldwide prompted the implementation of a range of preventive measures at local, national, and international levels. Early in the outbreak, before the vaccine became accessible, voluntary quarantine and social isolation emerged as crucial strategies to curb the spread of infection. In this research, we present a game-theoretic model to elucidate the voluntary disclosure of exposure to infected individuals within communities. By employing a fractional derivative approach to illustrate disease propagation within the compartmental model, we determine the minimum level of voluntary disclosure required to disrupt the chain of transmission and allow the epidemic to fade. Our findings suggest that higher transmission rates and increased perceived severity of infection change the externality of disclosing infected exposure, thereby contributing to a rise in the proportion of individuals opting for quarantine and reducing disease incidence. We estimate behavioural parameters and transmission rates by fitting the model to hospitalized cases in Chile, South America. Results from our paper underscore the potential for public health authorities to influence and regulate voluntary disclosure of infection during emerging outbreaks through effective risk communication, emphasizing the severity of the disease, and providing accurate information about hospital capacity to the public.

## 1. INTRODUCTION

The COVID-19 virus, which was first detected in China in December 2019 [43], caused an unrivaled worldwide outbreak of infections, with 95 million reported cases globally [27, 45]. World Health Organization (WHO) officials moved quickly to declare the COVID-19 pandemic a global health emergency in reaction to the worsening situation [37, 39]. Mandatory lockdowns, quarantines, self-isolation, and the wearing of masks were among the measures put in place by authorities at the beginning of the outbreak to restrict the spread of the virus [14, 56]. Clinical practices such as rigorous testing, quarantine measures, and close monitoring were also initiated [47, 77]. A critical shortage in hospital bed availability, along with a deficit in essential medical resources like oxygen and medication, marked a significant crisis [38, 70]. By the end of September 2020, India had reported over  $63 \times 10^5$  confirmed COVID-19 cases, exhibiting a range of symptoms from mild upper respiratory tract issues to severe conditions such as acute respiratory distress syndrome and multi-organ failure, necessitating intensive care.

Even though a relatively small percentage of patients required critical care services, the surge in cases quickly overwhelmed the healthcare system. In the beginning of the COVID epidemic in India, the Ministry of Health and Family Welfare (MoHFW) suggested that around 2.5% of patients needed intensive care, although this might be an underestimate

---

2020 *Mathematics Subject Classification.* Primary: 92-10; Secondary: 92-08, 92D30 .

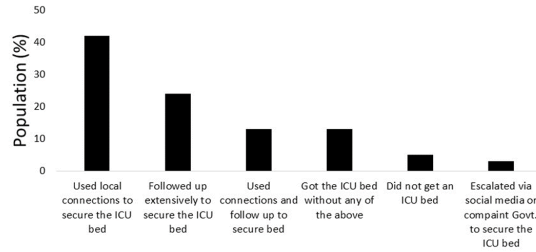


FIGURE 1. Impact of coronavirus (COVID-19) on securing ICU beds in hospitals across India as of April 2021 (Data source: [www.statista.com](http://www.statista.com))

due to incomplete reporting in some states [28]. As of June 28, 2020, the MoHFW reported 1,055 dedicated COVID hospitals in India, equipped with 177,529 isolation beds and 78,060 oxygen-supported beds. Additionally, there were 2,400 dedicated COVID Health Centres with 140,099 isolation beds and 51,371 oxygen-supported beds. However, this still left a considerable gap, with approximately 120,000 oxygen-supported beds available. It was estimated that 15% of patients, translating to about 1.5 million individuals in India, would require mild to moderate infection treatment with oxygen beds. Securing beds posed a significant challenge, as revealed by a Local Circles survey in April 2021 ([www.statista.com](http://www.statista.com)). Only 13% of respondents successfully obtained an ICU bed through the standard procedure, while the majority had to rely on personal connections. Overall, the survey indicated widespread difficulties in securing COVID ICU beds for family and friends (see Fig 1). In confronting the critical challenge of disease outbreak management, health authorities consistently advocate for voluntary adherence to quarantine measures, stressing the significance of individuals disclosing potential exposure and initiating self-quarantine protocols [79, 64]. However, the decision to comply with such directives involves intricate strategic deliberations at the individual level, weighing perceived benefits against associated costs, and encompassing economic ramifications and constraints on personal liberties [63, 61, 57]. To thoroughly examine the dynamic interaction between social distancing, quarantine compliance, and disease containment, researchers have increasingly turned to game-theoretic frameworks ([26] and references therein), especially in vaccination behaviour [10, 9], social-distancing [12], and self-medication of antibiotics [48] and ITN usages in malaria control [44]. By utilizing game theory concepts within epidemiological models, such as the SEIR model, A. Satapathi et al. [63] have investigated how individuals make decisions to safeguard themselves and engage with one another. This integration enables exploring diverse scenarios and behavioural responses to quarantine mandates. Game theory has been applied recently in many other fields of research. For example, B. Yan et al. [76] devised a game-theoretical model from the defender's standpoint, integrating attackers' resource consumption into the model. M. Ochab et al. [53] showcased a model of behavioural response, integrating it into the nonlinear feedback control theory framework.

During the COVID-19 outbreak, several distinct computational and mathematical models have been developed to investigate the significance of quarantine as a game-theoretic strategy for preventing the number of disease cases and the burden on hospitals [61, 49, 2, 41]. C. N. Ngonghala et al. [49] introduced two models inspired by the COVID-19 pandemic, incorporating elements of game theory, disease dynamics, human behaviour,

and economics. A study by A. Rajeev et al. [57] delved into an evolutionary game theory model aimed at examining individuals' behavioural patterns and identifying stable states. J. Tanimoto et al. [2] emphasized the significance of implementing multiple provisions promptly to enhance disease containment efforts using game theory and human behaviour. C. M. Saad-Roy et al. [61] investigated interconnected dynamics by integrating a game-theoretic model focused on individual adherence to non-pharmaceutical interventions (NPIs) within an epidemiological framework. H. Khazaei et al. [41] analyzed the SEIR epidemiological model alongside an individual behaviour response model, specifically exploring the dynamics of a game where the public's compliance with social distancing measures is influenced by the state of disease and associated payoffs. Using the fractional derivative method, several mathematical models have been constructed to account for modeling memory effects and long-range dependencies, often present in real-world epidemiological data [72, 78, 73]. With the two forms of immunity, artificial and natural immunity, taken into account, Mohammad Sharif Ullah et al. [72] provided a mean-field approximation and fractional-order model for the susceptible-vaccinated-infected-recovered (SVIR) epidemic dynamics. To examine the impact of individual vaccination on the monitoring of COVID-19 transmission, Akeem O. Yunus et al. [78] developed a fractional order model and analyzed it. Mubashara Wali et al. [73] introduced a novel numerical approach for the COVID-19 epidemic model based on the Atangana-Baleanu fractional order derivative in the Caputo sense to study vaccination efficacy. However, no study considers disclosing exposure to infection as an individual choice in the face of an outbreak and limited availability of medical facilities. Understanding the interplay between individual strategies and the availability of medical facilities, and its consequences on disease burden is an important challenge for public health policymakers.

In this study, we explore the interplay between individual decision-making and epidemiological factors by developing a game-theoretic model utilizing fractional-order derivatives. We have identified the critical level of disclosure necessary for the epidemic to fade out. We simulate and explore how the disease transmission rate and interventions in public health, or the severity of the disease, influence individuals' decisions. According to our results, the population exhibits higher disclosure tendencies due to the combined impact of transmission and disease severity. Our analysis underscores the importance of infection disclosure as a strategic decision and its implications for illness control and the burden of hospitalization.

## 2. MODEL FRAMEWORK

**2.1. Disease model.** We model the human population consisting of six distinct compartments: susceptible ( $S$ ), exposed ( $E$ ), infected ( $I$ ), quarantined ( $Q$ ), hospitalized ( $H$ ), and recovered ( $R$ ) with the total population ( $N$ ) is given by  $N = S + E + I + Q + H + R$ . Figure 2 displays the schematic of the disease model, and Table 1 describes parameters used in the model. Individuals in either the exposed or infected class can transmit the infection to susceptible individuals. Once exposed, individuals can choose to disclose their exposure to the infection based on certain perceived costs (discussed in the *Game-theory model* description below) associated with disclosing and non-disclosing. Whether quarantined or not, individuals may develop severe symptoms and subsequently be hospitalized (at a rate  $\alpha$ ), depending on public health authority preferences ( $\eta_q$ ), or they may recover

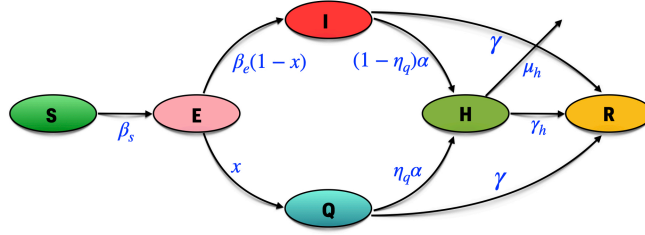


FIGURE 2. Schematic of the coupled disease game-theoretic model

from the infection. Additionally, there is a risk of disease-induced death among hospitalized patients. Below, we have the epidemiological model equations using the fractional order derivative approach:

$$\begin{aligned}
 {}^C_0 D_t^\zeta S &= \frac{-\beta_s(I+E)S}{N} \\
 {}^C_0 D_t^\zeta E &= \frac{\beta_s(I+E)S}{N} - xE - \beta_e(1-x)E \\
 {}^C_0 D_t^\zeta Q &= xE - \eta_q \alpha Q - \gamma Q \\
 {}^C_0 D_t^\zeta I &= \beta_e(1-x)E - (1-\eta_q)\alpha I - \gamma I \\
 {}^C_0 D_t^\zeta H &= (1-\eta_q)\alpha I + \eta_q \alpha Q - \gamma_h H - \mu_h H
 \end{aligned}
 \tag{2.1}$$

subject to initial condition:  $S(0) = S_0$ ,  $E(0) = E_0$ ,  $I(0) = I_0$ ,  $Q(0) = Q_0$ , and  $H(0) = H_0$ .  $\beta_s$  denotes the transmission rate and  $\beta_e$  denotes the incubation rate. We do not explicitly mention the recovery compartment  $R$  here in model equation (2.1), as individuals become completely immune after recovery and the population is closed.  $x$  represents the percentage of exposed individuals who choose to disclose of the exposure to infection and eventually be quarantined (see game-theoretic model below for description of  $x$ ).

**2.2. Game-theoretical model.** We classify this decision-making framework as a population game, where an individual's payoff is determined by their own behaviour as well as the collective behaviour of the community. The players are individuals who are exposed ( $E(t)$ ) to infection. Let  $x$  ( $0 \leq x \leq 1$ ) represent the fraction of the players who choose to disclose their infection and opt for quarantine. It might be interesting to note that players of the present generation compete not only with players of the previous generation but also with players from past generations who have similar behaviours since the individual choice relies on the current illness prevalence and availability of hospital treatment. We suppose that people imitate other individuals' behaviour, which is more likely for strategic decision-making in various social engagements. In particular, they adopt strategies from other members with a likelihood proportional to the projected pay-off increase if the sampled individual's pay-off is greater [35, 11]. It is presumed that individuals choose their strategy based on the perceived benefits of disclosing the infection and quarantine.

TABLE 1. Description of baseline parameters &amp; variables.

Parameters	Description
$\beta_s$	Mean disease transmission rate (per day)
$\beta_e$	Mean incubation rate (per day)
$\eta_q$	Preference by public health authorities to provide treatment facility
$\alpha$	Rate of hospital admissions (per day)
$\mu_h$	Mortality rate after hospitalization (per day)
$\zeta$	Order of fractional derivative
$\gamma$	Recovery rate from infection (per day)
$\gamma_h$	Recovery rate of hospitalized patients (per day)
$\kappa$	Sampling rate in social learning (per day)
$c_d$	Per unit cost of disclosing infection
$c_{nd}$	Per unit cost of non-disclosing infection
$p_s$	Probability of developing severity upon infection
Variables	Description
$N$	Total population
$S(t)$	Susceptible
$E(t)$	Exposed
$I(t)$	Infected
$Q(t)$	Quarantined
$H(t)$	Hospitalized
$R(t)$	Recovered
$x(t)$	Fraction of exposed population choosing disclosing infection and quarantine

In game theory, the players are assumed to maximize their payoff. We consider two strategies: *disclosing infection and opting for quarantine*, and *non-disclosing infection*. The perceived payoff of adopting a disclosure strategy is:

$$(2.2) \quad p_d = -c_d(1 - \eta_q)$$

where  $c_d$  is the per unit perceived cost of disclosing and isolation. We have also assumed the public health authority has preference in providing treatment facilities to individuals depending on disclosure to infection. During the beginning of the COVID-19 outbreak, there were many centralized isolation and quarantine facilities for patient observation and treatment [74, 82]. We introduced the parameter  $\eta_q$  to indicate preferences by public health authorities in providing treatment facilities to exposed individuals based on whether they disclose their status. We intend to analyze the impact of preferences by public health authorities on the disclosing game. Here, we simulate our model under both scenarios: with and without preferences by public health authorities in providing treatment (see results section).

The perceived payoff of adopting a non-disclosure strategy is:

$$(2.3) \quad p_{nd} = -c_{nd}p_s f(H)$$

where  $c_{nd}$ ,  $p_s$  are the perceived per unit cost of non-disclosing infection and the probability of developing severe infection, respectively. Individuals' perceptions of this factor are influenced by the number of current hospital admissions,  $H(t)$  in the community.  $f(H)$

is a function indicating that costs increase as  $H$  increases:

$$(2.4) \quad f(H) = \frac{H}{a + H}$$

where  $a$  is the half-saturation coefficient. The cost of non-disclosing of infection increases as  $H$  increases. So, the expected payoff gain upon changing the non-disclosing strategy to disclosing is:

$$(2.5) \quad \Delta E = p_d - p_{nd} = -c_d(1 - \eta_q) + c_{nd}p_s f(H)$$

All individuals are payoff maximizers, who randomly sample other population members and move to the strategy that provides them with the highest payoff. Thus, the time evolution of the frequencies of the disclosure strategy for an imitation game is as follows:

$$(2.6) \quad {}^C_0 D_t^\zeta x = \kappa x(1 - x)(-c_d(1 - \eta_q) + c_{nd}p_s f(H))$$

Here,  $\kappa$  is the sampling rate in social learning. This is similar to the replicator equation in evolutionary game theory [33, 8].

**2.3. Coupled disease game-theoretic model.** Combining the game-theoretic model (equation 2.6) and the epidemiological model (equation 2.1), we have:

$$(2.7) \quad \begin{aligned} {}^C_0 D_t^\zeta S &= \frac{-\beta_s(I + E)S}{N} \\ {}^C_0 D_t^\zeta E &= \frac{\beta_s(I + E)S}{N} - xE - \beta_e(1 - x)E \\ {}^C_0 D_t^\zeta Q &= xE - \eta_q \alpha Q - \gamma Q \\ {}^C_0 D_t^\zeta I &= \beta_e(1 - x)E - (1 - \eta_q)\alpha I - \gamma I \\ {}^C_0 D_t^\zeta H &= (1 - \eta_q)\alpha I + \eta_q \alpha Q - \gamma_h H - \mu_h H \\ {}^C_0 D_t^\zeta x &= \kappa x(1 - x)(-c_d(1 - \eta_q) + c_{nd}p_s f(H)) \end{aligned}$$

subject to the initial condition:

$$\begin{aligned} S(0) &= S_0, E(0) = E_0, I(0) = I_0, Q(0) = Q_0, \\ H(0) &= H_0, x(0) = x_0 \end{aligned}$$

We evaluate and computationally simulate this model (equation 2.7) to learn how changing behavioural and epidemiological characteristics affect the dynamics of a disease prevalence.

### 3. PRELIMINARIES

Let  $f$  be a real-valued differentiable function. The  $n^{th}$  Cauchy repeated integral formula gives an expression for compressing  $n \in \mathbb{N}$  repeated integrals of  $f$  into a single antiderivative on an interval with base point  $a$ , which is given by [3]:

$${}_a J_t^n f(t) = \frac{1}{n!} \int_a^t (t - s)^{n-1} f(s) ds.$$

This is useful in finding analogous expressions for the integral of  $f$  when  $n$  is not an integer. So, the Riemann-Liouville fractional integral of  $f$  of order  $\zeta > 0$ , where  $\zeta \in \mathbb{R}^+$  is given by [21]:

$${}_a J_t^\zeta f(t) = \frac{1}{\Gamma(\zeta)} \int_a^t (t-s)^{\zeta-1} f(s) ds.$$

for  $t > a$ , where  $\Gamma(\zeta)$  is the Gamma function evaluated at  $\zeta$ . The fractional derivative of  $f$  of order  $\zeta$  is based upon the Riemann-Liouville integral definition, making fractional derivatives a non-local property. This non-local property is particularly advantageous, as it proves to provide more accurate numerical solutions for phenomena that can be modelled by fractional differential equations [7, 36]. Denoting  $n = \lfloor \zeta \rfloor$  to be the greatest integer closest to  $\zeta$ , The Riemann-Liouville fractional derivative is given by:

$${}_a D_t^\zeta f(t) = \frac{d^n}{dt^n} \left( {}_a J_t^{n-\zeta} f(t) \right).$$

Other commonly used definitions of the fractional derivative include the Caputo-fractional derivative [81], which is given by:

$${}_0^C D_t^\zeta f(t) = \frac{1}{\Gamma(n-\zeta)} \int_0^t \frac{f^{(n)}(s)}{(t-s)^{\zeta+1-n}} ds.$$

Differential equations involving derivatives of rational orders can be defined, and most series solutions to these equations are obtained by applying Laplace and inverse Laplace transforms [3]. Due to the non-linear nature of our model given by equation (2.7), numerical techniques of approximating the solutions prove to be of greater utility, as compared to analytical solutions. Various methods such as the fractional Euler method [66], and the generalized Runge-Kutta scheme have been proposed [80], but we shall be using the Adams-Bashfourth-Moulton predictor-corrector method which gives an elegant way of iteratively solving a fractional differential equation subject to the initial conditions [58].

As this method is iterative, we work with a uniform grid having increment step  $h$ , which may be chosen as  $h = T/N$ , where  $T$  is the time span and  $N$  is a natural number. We compute the value of the differential equation at step  $t_{n+1}$ , assuming the value at  $t_n$  is known [21].

In the ordinary first-order differential equation,  $Dy(t) = f(t, y(t))$  subject to  $y(0) = y_0$ , the classical one-step method gives the solution as follows:

$$y(t_{n+1}) = y(t_n) + \int_{t_n}^{t_{n+1}} f(z, y(z)) dz$$

In order to compute this integral, we apply the trapezoidal rule which gives [42, 40]:

$$y(t_{n+1}) = y(t_n) + \frac{h}{2} (f(t_n, y(t_n)) + f(t_{n+1}, y(t_{n+1})))$$

However, the term on the right-hand side includes the values at  $t_{n+1}$ , which is unknown to us. In this case, we make a prediction of the value,  $y^*(t_{n+1})$ , which is obtained by the rectangle rule as:

$$y^*(t_{n+1}) = y(t_n) + h f(t_n, y(t_n))$$

So, the one-step method may be summarized as:

$$y(t_{n+1}) = y(t_n) + \frac{h}{2} (f(t_n, y(t_n)) + f(t_{n+1}, y^*(t_{n+1})))$$

We define an analogous scheme in the fractional setup. Let the fractional differential equation of order  $\zeta \in \mathbb{R}^+$  be given by [20]:

$$D^\zeta y(t) = f(t, y(t))$$

subject to  $y(t_0) = y_0$ . The solution to this differential equation is given by the Volterra-integral equation which may be represented as:

$$y(t) = y(0) + \frac{1}{\Gamma(\zeta)} \int_0^t (t-s)^{\zeta-1} f(s, y(s)) ds$$

Notice here that the integration starts from 0 to  $t$ , due to the non-local nature of the fractional derivative. So, the iterative step translates the Volterra equation into [20]:

$$y(t_{n+1}) = y(0) + \frac{1}{\Gamma(\zeta)} \int_0^{t_{n+1}} (t_{n+1} - z)^{\zeta-1} f(z, y(z)) dz$$

To compute this integral, we make the following approximation:

$$\int_0^{t_{n+1}} (t_{n+1} - z)^{\zeta-1} f(z, y(z)) dz = \frac{h^\zeta}{\zeta(\zeta+1)} \sum_{j=0}^{n+1} a_{j,n+1} f(t_j, y(t_j)).$$

where  $a_{j,n+1}$  is a weight function given by:

$$a_{j,n+1} = \begin{cases} n^{\zeta+1} - (n-\zeta)(n+1)^\zeta & j=0 \\ (n-j+2)^{\zeta+1} + (n-j)^{\zeta+1} - 2(n-j+1)^{\zeta+1} & 1 \leq j \leq n \\ 1 & j=n+1. \end{cases}$$

So, the analogous predictor-corrector method can be obtained by solving the approximation using the weight functions and putting it into the Volterra equation. This gives:

$$y(t_{n+1}) = y(0) + \frac{h^\zeta}{\Gamma(\zeta)} \left[ f(t_{n+1}, y^*(t_{n+1})) + \sum_{j=0}^{n+1} a_{j,n+1} f(t_j, y(t_j)) \right].$$

In order to approximate the predicted value, we use the rectangle rule of integration and add suitable weights  $b_{j,n+1}$  which gives:

$$y^*(t_{n+1}) = y(0) + \frac{1}{\Gamma(\zeta)} \sum_{j=0}^{n+1} b_{j,n+1} f(t_j, y(t_j))$$

where  $b_{j,n+1} = \frac{h^\zeta}{\zeta} ((n+1-j)^\zeta - (n-j)^\zeta)$ .

Hence, the Adams-Moulton predictor-corrector method for fractional derivatives can be summarized into:

$$(3.1) \quad \begin{aligned} y(t_{n+1}) = & y(0) + \\ & \frac{h^\zeta}{\Gamma(\zeta)} \left[ f \left( t_{n+1}, y(0) + \frac{1}{\Gamma(\zeta)} \sum_{j=0}^{n+1} b_{j,n+1} f(t_j, y(t_j)) \right) \right. \\ & \left. + \sum_{j=0}^{n+1} a_{j,n+1} f(t_j, y(t_j)) \right]. \end{aligned}$$



#### 4. RESULTS

**4.1. Equilibria, Reproduction numbers and Stability analysis.** We have the disease-free equilibrium and the disease-endemic equilibrium. Depending on whether individuals opt for disclosing or not, there are mainly two important disease-free equilibria:  $E_1^d = (N, 0, 0, 0, 0, 0)$  and  $E_2^d = (0, 0, 0, 0, 0, 1)$ . We call  $E_1^d$  a purely non-disclosing game, and  $E_2^d$  a purely disclosing game. We compute the basic reproduction ratio, the control reproduction ratio, and the Jacobian matrix near the disease-free equilibrium  $E_1^d$ . This gives the optimal fraction of disclosing individuals needed to contain the disease in the near future.

**4.1.1. Basic reproduction number  $R_0$  when  $x = 0$ .** In the case when  $x = 0$ , the reproduction number  $R_0$  is given by the dominant eigenvalue of the next-generation method as follows:

The infected classes for this system will be:

$$\begin{aligned} {}^C_0 D_t^\zeta E(t) &= \frac{\beta_s(I+E)S}{N} - \beta_e E \\ {}^C_0 D_t^\zeta I(t) &= \beta_e E - (1 - \eta_q)\alpha I - \gamma I \end{aligned}$$

So:

$$\begin{aligned} f &= \begin{bmatrix} \frac{\beta_s(I+E)S}{N} \\ 0 \end{bmatrix}, v = \begin{bmatrix} -\beta_e E \\ \beta_e E - \gamma I - (1 - \eta_q)\alpha I \end{bmatrix} \\ F &= \begin{bmatrix} \frac{\beta_s S}{N} & \frac{\beta_s S}{N} \\ 0 & 0 \end{bmatrix}, V = \begin{bmatrix} -\beta_e & 0 \\ \beta_e & -(\gamma + (1 - \eta_q)\alpha) \end{bmatrix} \\ V^{-1} &= \frac{1}{\beta_e((1 - \eta_q)\alpha + \gamma)} \begin{bmatrix} -(\gamma + (1 - \eta_q)\alpha) & 0 \\ -\beta_e & -\beta_e \end{bmatrix} \\ \Rightarrow FV^{-1} &= \frac{1}{\beta_e((1 - \eta_q)\alpha + \gamma)} \begin{bmatrix} \frac{-(\gamma + (1 - \eta_q)\alpha)\beta_s S - \beta_e \beta_s S}{N} & \frac{-\beta_e \beta_s S}{N} \\ 0 & 0 \end{bmatrix} \end{aligned}$$

The dominant eigenvalue of the next generation matrix  $[FV^{-1}]$  is:

$$R_0(S, N) = \frac{\beta_s S}{\beta_e N} + \frac{\beta_s S}{((1 - \eta_q)\alpha + \gamma)N}$$

Evaluating this at the disease-free equilibrium point

$E^{df}(S^{df}, E^{df}, I^{df}, Q^{df}, H^{df}) = (N, 0, 0, 0, 0)$  gives the reproduction number  $R_0$ :

$$R_0 = \beta_s \left[ \frac{1}{\beta_e} + \frac{1}{((1 - \eta_q)\alpha + \gamma)} \right].$$

**4.1.2. Control reproduction number  $R_c$  when  $x \neq 0$ .** The control reproduction number  $R_c$  is obtained similarly, computed as follows:

The Infected classes are:

$$\begin{aligned} {}^C_0 D_t^\zeta E(t) &= \frac{\beta_s(I+E)S}{N} - xE - \beta_e(1-x)E \\ {}^C_0 D_t^\zeta I(t) &= \beta_e(1-x)E - (1 - \eta_q)\alpha I - \gamma I \end{aligned}$$

So:

$$f = \begin{bmatrix} \frac{\beta_s(I+E)S}{N} \\ 0 \end{bmatrix}, v = \begin{bmatrix} -xE - \beta_e(1-x)E \\ \beta_e(1-x)E - \gamma I - (1 - \eta_q)\alpha I \end{bmatrix}$$

$$\begin{aligned}
F &= \begin{bmatrix} \frac{\beta_s S}{N} & \frac{\beta_s S}{N} \\ 0 & 0 \end{bmatrix}, V = \begin{bmatrix} -x - \beta_e(1-x) & 0 \\ \beta_e(1-x) & -((1-\eta_q)\alpha + \gamma) \end{bmatrix} \\
\Rightarrow V^{-1} &= \frac{1}{(x+\beta_e(1-x))((1-\eta_q)\alpha + \gamma)} \times \\
&\quad \begin{bmatrix} -(\gamma + (1-\eta_q)\alpha) & 0 \\ -\beta_e(1-x) & -(x + \beta_e(1-x)) \end{bmatrix} \\
\Rightarrow FV^{-1} &= \frac{1}{(x+\beta_e(1-x))((1-\eta_q)\alpha + \gamma)} \times \\
&\quad \begin{bmatrix} \frac{-(\beta_s S)*((1-\eta_q)\alpha + \gamma) - \beta_e(1-x)\beta_s S}{N} & \frac{-(x+\beta_e(1-x))\beta_s S}{N} \\ 0 & 0 \end{bmatrix}
\end{aligned}$$

Thus, the dominant eigenvalue of the next-generation matrix  $[FV^{-1}]$  is:

$$R_c(x) = \frac{\beta_s S}{(x + \beta_e(1-x))N} + \frac{\beta_e \beta_s (1-x)S}{(x + \beta_e(1-x))((1-\eta_q)\alpha + \gamma)N}.$$

Evaluating this at the disease-free equilibrium point  $E_1^d$ , gives the control-reproduction number  $R_c$  as a function of  $x$ :

$$R_c(x) = \frac{\beta_s}{(x + \beta_e(1-x))} \left[ 1 + \frac{\beta_e(1-x)}{((1-\eta_q)\alpha + \gamma)} \right].$$

The disease-free equilibrium is stable if  $R_c < 1$ , which implies

$$(4.1) \quad x_c > \frac{((1-\eta_q)\alpha + \gamma)(\beta_s - \beta_e) + \beta_s \beta_e}{\beta_s \beta_e + (1 - \beta_e)((1-\eta_q)\alpha + \gamma)}$$

This indicates that it requires at least an  $x_c$  proportion of individuals to disclose their exposure of infection for the infection in the population to die out immediately.

We also compute the Jacobian matrix of the system at  $E_1^d$ :

$$J^d = \begin{bmatrix} \frac{-\beta_s(I+E)}{N} & \frac{-\beta_s S}{N} & 0 & \frac{-\beta_s S}{N} & 0 & 0 \\ \frac{\beta_s(I+E)}{N} & \frac{\beta_s S}{N} - x - \beta_e(1-x) & 0 & \frac{\beta_s S}{N} & 0 & -E + \beta_e E \\ 0 & x & -\eta_q \alpha - \gamma & 0 & 0 & E \\ 0 & \beta_e(1-x) & 0 & -(1-\eta_q)\alpha - \gamma & 0 & -\beta_e E \\ 0 & 0 & \eta_q \alpha & (1-\eta_q)\alpha & 0 & 0 \\ 0 & 0 & 0 & 0 & -\frac{\gamma_h + \mu_h}{(a+H)^2} & (1-2x)\kappa \Delta E \end{bmatrix}$$

Substituting the values of equilibrium component into the Jacobian matrix, we get:

$$J^d = \begin{bmatrix} 0 & -\beta_s & 0 & -\beta_s & 0 & 0 \\ 0 & \beta_s - \beta_e & 0 & \beta_s & 0 & 0 \\ 0 & 0 & -\eta_q \alpha - \gamma & 0 & 0 & 0 \\ 0 & \beta_e & 0 & -(1-\eta_q)\alpha - \gamma & 0 & 0 \\ 0 & 0 & \eta_q \alpha & (1-\eta_q)\alpha & -\gamma_h - \mu_h & 0 \\ 0 & 0 & 0 & 0 & 0 & -\kappa C_d(1-\eta_q) \end{bmatrix}$$

It has the following eigenvalues:

$$\lambda_1 = 0, \lambda_2 = -\eta_q \alpha - \gamma, \lambda_3 = -\gamma_h - \mu_h, \lambda_4 = -\kappa C_d(1-\eta_q).$$

Other two eigenvalues are represented by the following quadratic equation in  $\lambda$ :

$$\begin{aligned}
\lambda^2 - \lambda [(\beta_s - \beta_e) - ((1-\eta_q)\alpha + \gamma)] + \\
[\beta_s \beta_e - (\beta_s - \beta_e)((1-\eta_q)\alpha + \gamma)] &= 0.
\end{aligned}$$

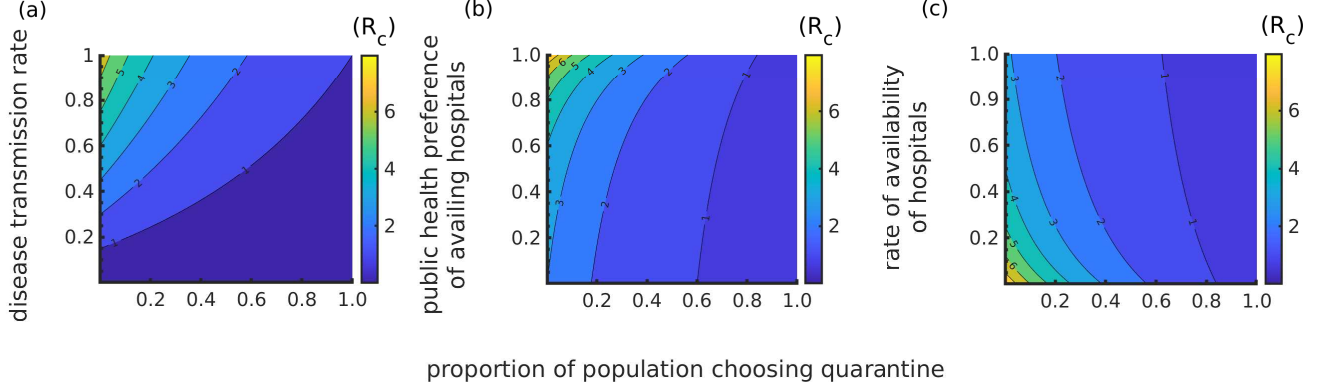


FIGURE 3. Control reproduction number ( $R_c$ ) of the model for different values of  $0 \leq x \leq 1$  on the x-axis with (a)  $0 < \beta_s < 1$  (b)  $0 \leq \eta_q \leq 1$  (c)  $0 \leq \alpha \leq 1$  on the y-axis.

The following sufficient criterion ensures that these eigenvalues are also negative:

$$\beta_s - \beta_e < \min\{\sqrt{\beta_s \beta_e}, (1 - \eta_q)\alpha + \gamma\}$$

This however, indicates the stability of the disease-free equilibrium  $E_1^d$ .

We have further plotted the control reproduction number  $R_c$  as a function of  $x$  and other important parameters such as  $\beta_s$  (the transmission rate),  $\eta_q$  (public health preference in providing hospital beds), and  $\alpha$  (rate of hospital beds in the community) (Figure 3). This figure clearly shows that higher values of  $x$  reduce the force of infection in the transmission of the disease (Figure 3(a)). Also, higher availability of hospital beds in the community or even relatively low preference in accessing hospitals among individuals with disease will die out immediately with a lower proportion of disclosing (Figure 3(b & c)). This happens because the infected individuals once hospitalized, are isolated and reduce the transmission. This indicates that a greater supply of beds in the community might help reduce the transmission of infection. We will now simulate the model using several parameters under baseline values to analyze the impact of disclosing infection on the dynamics of disease spread.

## 5. NUMERICAL SIMULATION

We simulated the FDE model (2.7) with the values of parameters described in Table 2. As discussed in Section 3, we have described that we have used the Adams-Bashfourth-Moulton predictor-corrector method for simulating the model. The initial population distributions are as follows:  $S(0) = 50000$ ;  $E(0) = 500$ ;  $I(0) = 100$ ;  $Q(0) = 20$ ;  $H(0) = 0$ ;  $R(0) = 0$ ; and  $x(0) = 0.15$ .

TABLE 2. Baseline values (or ranges) of the parameters.

Parameter	$\beta_s$	$\beta_e$	$\eta_q$	$\alpha$	$\mu_h$	$\zeta$	$\gamma$	$\gamma_h$	$\kappa$	$c_d$	$c_{nd}$	$p_s$
Values/Ranges	0.6	0.3	(0-1)	(0-1)	0.3	0.9	0.1	0.071	(0-1)	(0-1)	(0-1)	(0-1)
Ref.	[32]	[52]			[51]	[4]	[15]	[68]				

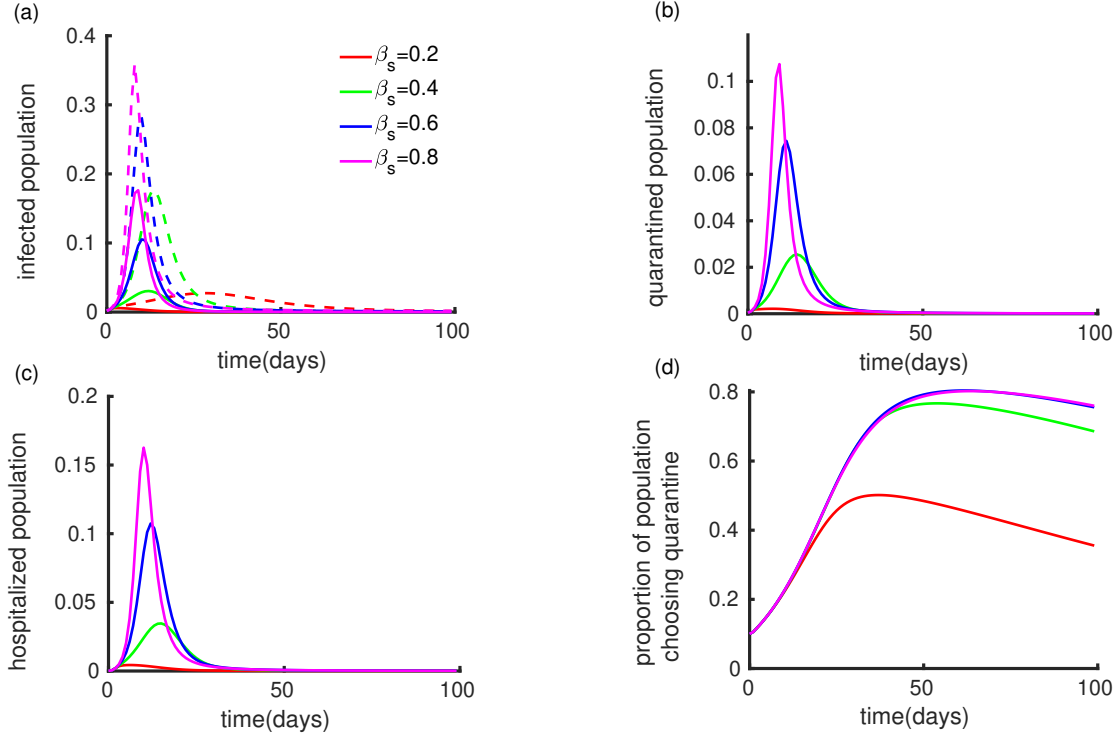


FIGURE 4. The dynamics of different trajectories of the model: (a) infected population, (b) quarantine population (c) hospitalized, and (d) proportion  $x$  of individuals who choose to disclose their infection for different values of transmission rate ( $\beta_s$ ) results, with  $c_d = 0.05$ ,  $c_{nd} = 0.2$ ,  $\kappa = 0.5$ ,  $a = 2000$ , and  $p_s = 0.8$ . In figure (a), the dotted line indicates the dynamics of infected population when  $x = 0$ . For details, see the text.

**5.1. Impact of rate of disease transmission rate ( $\beta_s$ ) and public health intervention ( $\eta_q$ ) on disease prevalence.** Transmission rate of infection ( $\beta_s$ ) and disease burden are important factors behind individuals decision to adopt quarantine [6, 34]. Figure 4 depicts the proportion of individuals in different compartments for sample values of  $\beta_s$ . A relatively small value of  $\beta_s = 0.2$  would mean a smaller fraction of individuals moving to the exposed compartment daily, subsequently leading to fewer infections, quarantines, and hospitalizations (red curve in Figures 4 (a),(b),(c)). Whereas, for a larger value of  $\beta_s = 0.8$ , the force of infection increases, causing an increase in the number of individuals in all compartments (pink curve in Figures 4 (a),(b),(c)). As the value of  $\beta_s$  increases, a greater number of individuals will be exposed. More and more individuals in the exposed compartment can utilize quarantine as its population rises. As a result, a

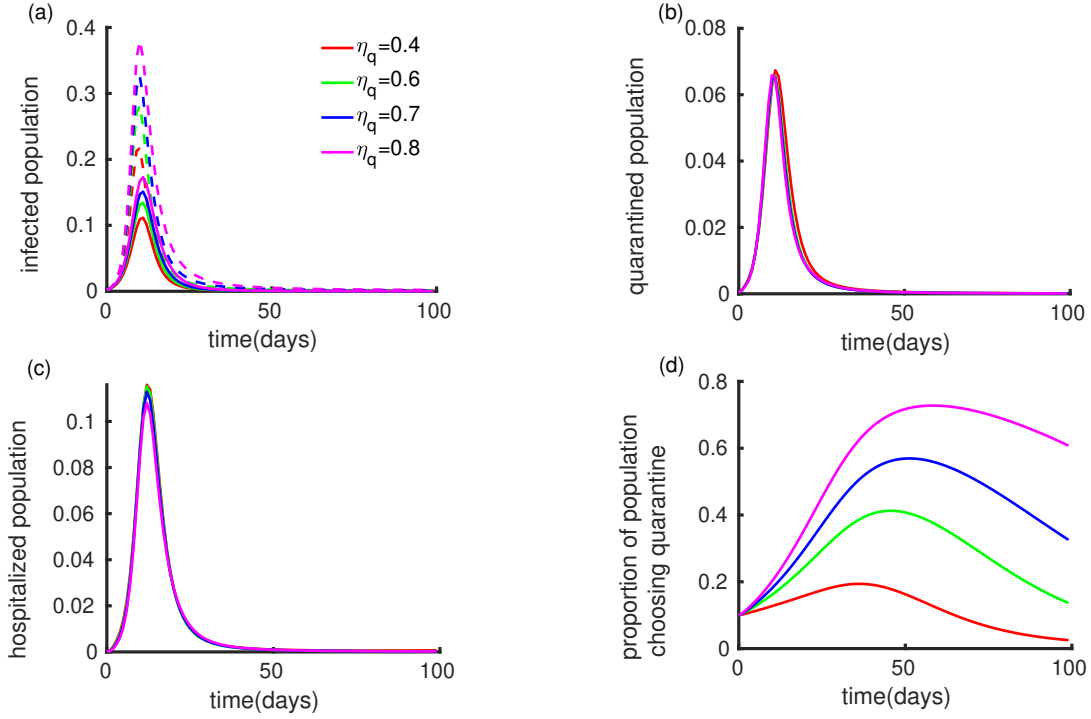


FIGURE 5. The dynamics of disease component of disease: (a) infected population, (b) quarantine population (c) hospitalized, and (d) proportion  $x$  of individuals who choose to disclose their infection under different values of preference to treatment facility rate ( $\eta_q$ ), with  $c_d = 0.2$ ,  $c_{nd} = 0.2$ ,  $\kappa = 0.5$  and  $p_s = 0.8$ . In figure (a), the dotted line indicates the dynamics of infected population when  $x = 0$ . For details, see the text.

higher value, such as  $\beta_s = 0.8$ , results in a higher percentage of people preferring quarantine than a lower value, such as  $\beta_s = 0.2$  &  $0.4$  (Figure 4 (b)). There are two important observations in this simulation: The first is the stark difference in the transmission profile of infection in the presence and absence of disclosing options (Figure 4 (a), dotted lines). The cumulative difference between these two indicates that disclosing exposure to infected neighbors may help reduce infection transmission in two ways: first, by improving hospital bed management, and second, by eventually isolating them from the general population, lowering the risk of infection transmission. The second observation is that the proportion of disclosing individuals at  $\beta_s = 0.2$  is significantly lower than the cases when  $\beta_s = 0.4$  or higher (Figure 4 (d)). Due to the high population in the infected and quarantined compartment for  $\beta_s = 0.8$  (Figure 4 (a & b)), the probability of acquiring a severe disease is high. Consequently, when  $\beta_s = 0.8$  as opposed to the low values ( $\beta_s = 0.2$  &  $0.4$ ), a large hospitalized population can be seen (Figure 4 (c)). Hence, the burden of surrounding infections directly influences this decision strategy. As a result, people choose to disclose information. One of the public health measures during the COVID-19 epidemic was to provide priority access to hospital facilities for people who voluntarily entered quarantine [22, 29]. In Figure 5, we see how public health interventions for providing hospitals to confined persons change over time for a range of  $\eta_q$  values. A higher value of  $\eta_q$  indicates a

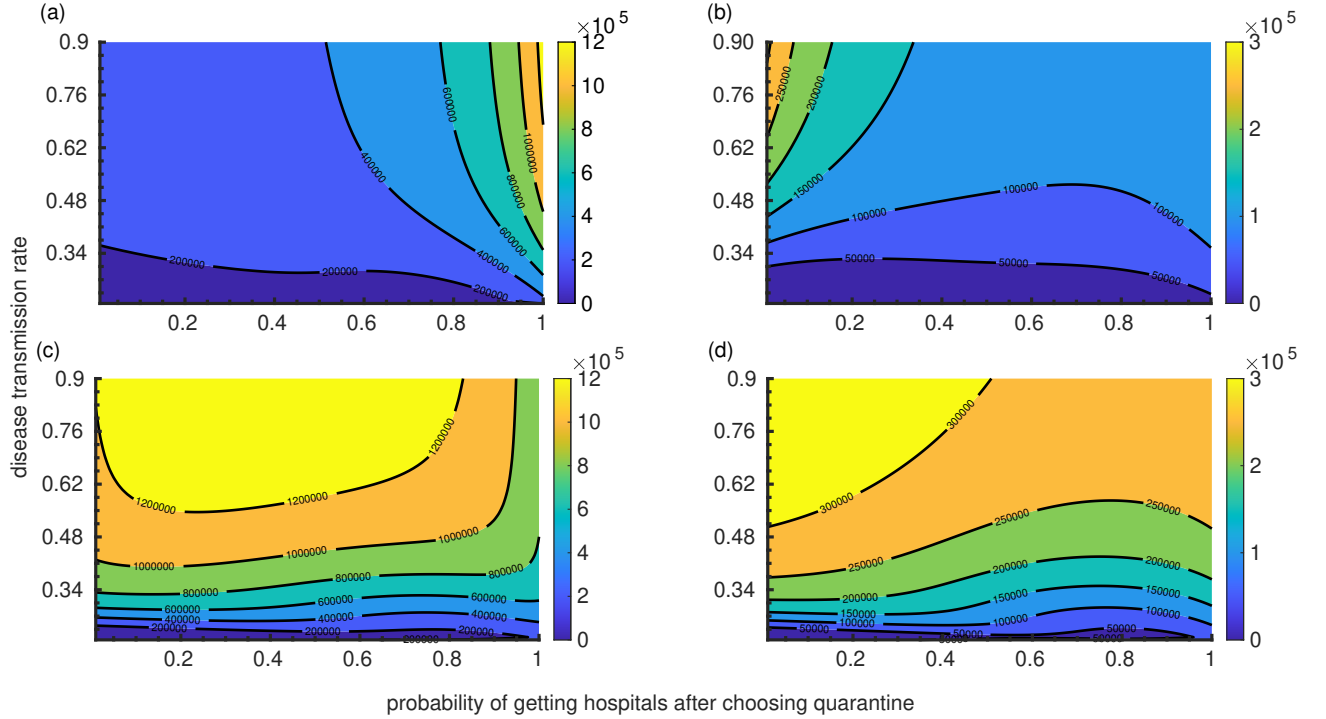


FIGURE 6. Figure represents the (a) cumulative infection (b) cumulative quarantined (c) cumulative hospitalized (d) cumulative quarantined population per day; as a function of probability of getting hospitals after choosing quarantine ( $\eta_q$ ) and transmission rate ( $\beta_s$ ), with  $c_d = 0.2$ ,  $c_{nd} = 0.2$ ,  $\kappa = 0.5$  and  $p_s = 0.8$ .

higher probability of getting hospital facilities for quarantined individuals. This, however, works as an incentive for the exposed individuals. On the other hand, a lower  $\eta_q$  discourages quarantine. This has been reflected in the dynamics of the quarantine population (Figure 5 (d)). However, it does not reflect in the population of the  $Q$  compartment (Figure 5 (b)). It is because individuals are also moving to the  $H$  compartment as  $\eta_q$  is higher. Nevertheless, this does not change much in the dynamics of disease (Figure 5 (a)). Because higher  $\eta_q$  values decrease the chance of getting a hospital facility for infected individuals who do not choose the strategy of disclosing their infection. Of course, with and without disclosing exposure show a similar difference as earlier (Figure 4). This analysis indicates important information for public health policymakers: more hospital facilities to individuals who choose to be quarantined may not help in reducing the infection in population a great extent.

Despite these results, the disease may be controlled by a combination of disease prevalence, burden, and public health initiatives. These factors will make individuals more likely to play with quarantine strategies. The combined influence of these two significant epidemiological factors is summarized in Figure 6. As previously observed, greater  $\beta_s$  values increase the disease burden, resulting in a large number of hospitalized patients (Figure 4 (a & c)). Whereas, an increased population hospitalization rate is associated

with a low  $\eta_q$  value (Figure 5 (c)). For  $0.2 \leq \eta_q \leq 0.5$  and  $\beta_s \geq 0.75$ , cumulative hospitalization is extremely high (Figure 6(c)). Because, as  $\eta_q$  is low,  $1 - \eta_q$  will be high, and for a high  $\beta_s$  value, the population will have the highest cumulative infection rate (Figure 6(a)). As a consequence of this, hospitals will accommodate the greatest number of patients possible (Figure 6(c)). For  $\eta_q \geq 0.899$  and  $\beta_s \geq 0.5456$ , the number of individuals choosing quarantine is very high (Figure 6(d)) because, for the same values, the cumulative exposed population is very large. As  $\eta_q$  has a high value,  $x$  will also be large (Figure 5(d)). Consequently, there may be a large number of people who are isolated and have high  $\eta_q$  &  $\beta_s$  values, which is reflected in the infection plot (Figure 6(a)). Large populations of the quarantined will enter the hospital section for a similar value of  $\eta_q$  &  $\beta_s$ , reducing the cumulative quarantine (Figure 6(b)). We analyzed the difference between the baseline payoff of disclosure and the new payoff of disclosure without  $1 - \eta_q$  to figure out the importance of public health measures (Figure 6 & S1). We can see that the cumulative infection with our baseline payoff is  $\approx 7 \times 10^5$  for  $\eta_q \geq 0.899$  and  $\beta_s \geq 0.546$  (Figure 6(a)); however, without  $1 - \eta_q$ , public health intervention does not affect infection; cumulative infection varies mainly owing to  $\beta_s$  (Figure S1). In fact, if there is a high transmission rate, public health efforts may help control the disease. As seen in the figure 6(d), the number of people choosing quarantine per day is similarly influenced by both epidemiological parameters simultaneously ( $\approx 5 \times 10^4$  for  $\eta_q \geq 0.899$  and  $\beta_s \geq 0.41$ ), whereas in Figure S1(d), the  $\beta_s$  value has the greatest impact.

Our research suggests that the public health intervention of providing hospitals for quarantine has a favorable effect on the quarantine and hospital burden if the disease transmission rate is high in the community. Additionally, this can help reduce the prevalence of disease in the population. During a pandemic, public health agencies may implement measures that mitigate the effects of the disease on the general population.

**5.2. Influence of incubation rate ( $\beta_e$ ) and probability of perceived severity ( $p_s$ ) on the disease.** The rate of developing disease ( $\beta_e$ ) after exposure to infection may play a certain role in disease dynamics. In Figure 7(a), a low value of  $\beta_e = 0.2$  corresponds to a lesser contribution to the infected class (red curve), while a higher value of  $\beta_e = 0.5$  would mean a greater contribution (pink curve). The game-theoretic equation that describes the change in the proportion of individuals opting to quarantine entirely depends on the payoff gain of disclosing, the probability of severity of infection, the public health initiative  $\eta_q$ , and the function of availability of hospital beds, as given in the replicator equation. Hence, due to the independence of  $\beta_e$ , different values of  $\beta_e$  do not affect the decision strategy of disclosing the infection at the onset of the disease, resulting in the same graph (Figure 7(d)). However, given this situation, a change in the proportion of quarantined individuals still occurs, as reflected in 7(b). This is because for a fixed value of  $\beta_s$ , the number of individuals in the exposed compartment is initially constant. Then, on the basis of non-disclosure, individuals move into the infection compartment at the rate of  $\beta_e$ , leaving a fraction of individuals to move into quarantine by disclosing. So, a lower value of  $\beta_e = 0.2$  would correspond to an increase in the number of individuals deciding to move into quarantine, as shown by the red curve in Figure 7(b). Similarly, higher values of  $\beta_e$  would lead to a decreased fraction of individuals opting for quarantine (red, green, and blue curves in Figure 7(b)). A change in the quarantined population also occurs due to the exit of individuals from the quarantined compartment to the hospitalized and recovered compartments, as given by our model. Yet again, the number of hospitalizations

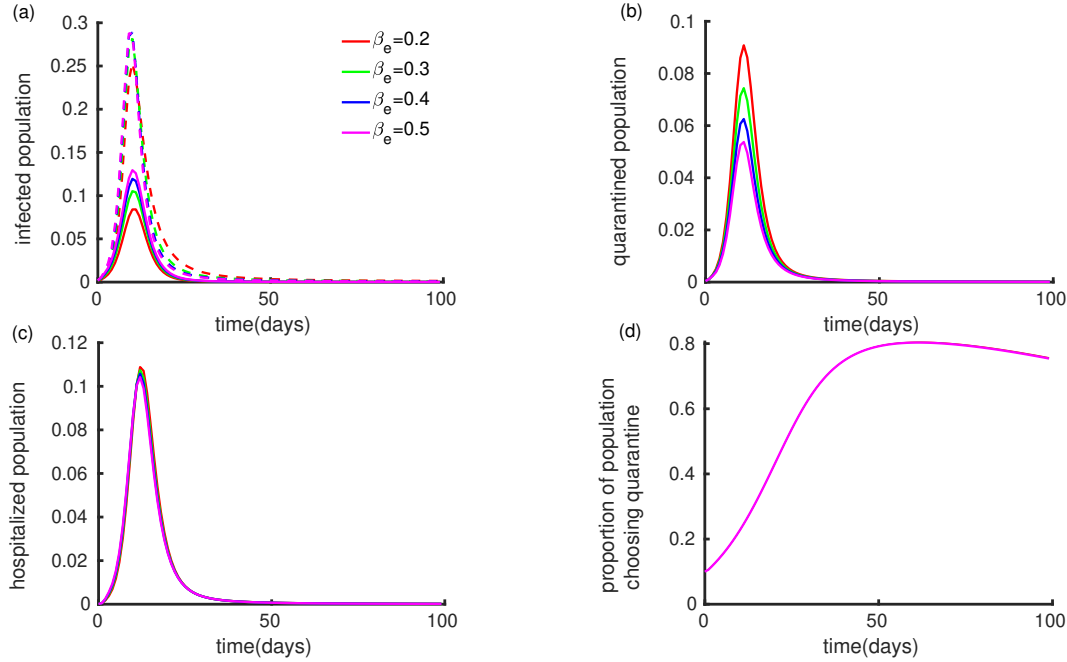


FIGURE 7. The dynamics of different trajectories of the model: (a) infected population, (b) quarantine population (c) hospitalized, and (d) proportion  $x$  of individuals who choose to disclose their infection for different values of incubation rate ( $\beta_e$ ) results, with  $c_d = 0.05$ ,  $c_{nd} = 0.2$ ,  $\kappa = 0.5$  and  $p_s = 0.8$ . In figure (a), the dotted line indicates the dynamics of infected population when  $x = 0$ . For details, see the text.

remains the same as seen in Figure 7(c) due to the constancy of  $x$  (Figure 7(d)) and its independence of  $\beta_e$ . Adopting a quarantine approach is heavily influenced by the relative probability of perceived severe symptoms after getting an infection [46, 18]. Figure 8 shows the interplay of severity of disease and quarantine for different values of  $p_s$ . When the probability of perceived severity is very high, i.e.,  $p_s = 1$ , more individuals prefer to adopt quarantine by disclosing their infection (pink curve in Figure 8 (d),(b)). Similarly, lesser values of  $p_s$ , such as 0.4 reflect a relatively lesser proportion of individuals disclosing their infection, hence causing a reduction in the number of individuals in the quarantined compartment (red curve in Figure 8 (d),(b)). Also, a higher proportion of individuals preferring to quarantine in the face of a greater probability of severity would mean a lesser proportion of individuals non-disclosing and hence moving into the infected compartment (pink curve in Figure 8 (a)). Likewise, a lesser severity of disease would correspond to a larger proportion of individuals feeling the need to disclose, causing an increase in infections (red curve in Figure 8 (a)). However, the number of hospitalizations remains unaffected in any scenario of severity, as seen in Figure 8 (c). The availability of hospital beds relies on  $\eta_q$ , which has no direct dependence on this probability. So, the probability of displaying severe symptoms has a direct impact on infections and the decision strategy of disclosure, but not on hospitalization proportions. These results show that the infection rate influences the number of people in quarantine, but has no effect on the fraction of people choosing quarantine at any given time. However, if the patient develops a severe



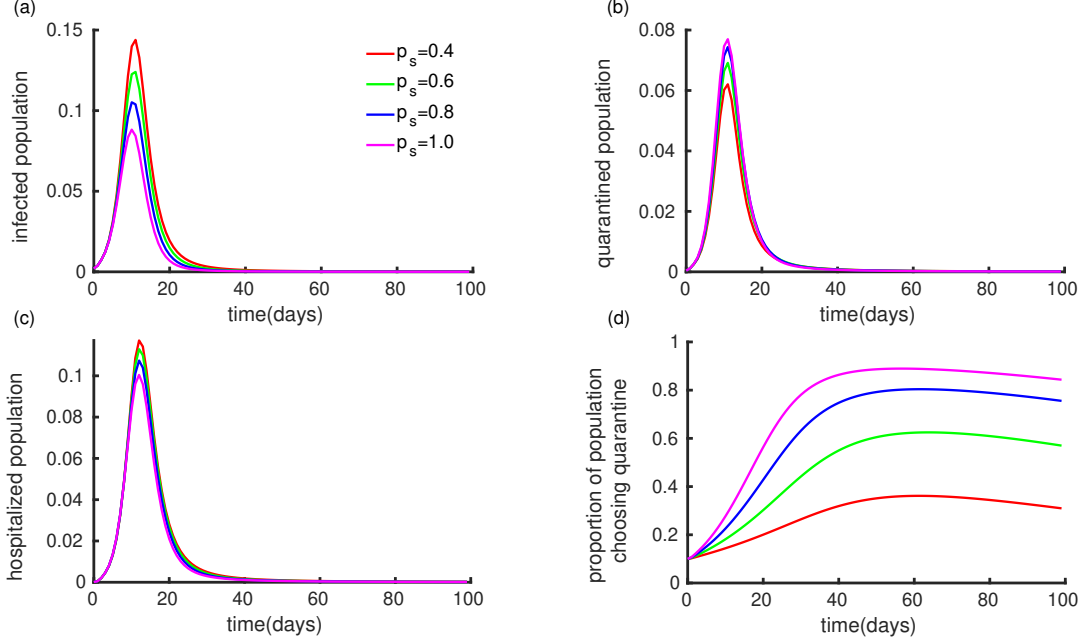


FIGURE 8. The dynamics of different trajectories of the model: (a) infected population, (b) quarantine population (c) hospitalized, and (d) proportion  $x$  of individuals who choose to disclose their infection for different probability of developing severity upon infection ( $p_s$ ) results, with  $c_d = 0.05$ ,  $c_{nd} = 0.2$ , and  $\kappa = 0.5$ . For details, see the text.

illness, the proportion of people who are able to make decisions shifts dramatically. Our findings may prompt public health officials to take action in response to the outbreak by ordering more isolation units to be built.

**5.3. Impact of probability of perceived severity ( $p_s$ ) with preference by public health authorities to provide treatment facilities ( $\eta_q$ ).** We simulate our model for various  $p_s$  and  $\eta_q$  values to see how they simultaneously affect illness prevalence and hospital burden. Figure 9 summarizes this. For  $p_s = 0$ , low values of  $\eta_q$  indicate that a large proportion of the population will opt for quarantine per day (Figure 9 (d)). As the value of  $p_s$  rises, people will fairly play with the strategy and make decisions to maximize their payoffs. For  $p_s \geq 0.899$  and  $\eta_q \geq 0.899$  (Figure 9 (d)), a large fraction of the population will engage in the decision-making process, which tends to result in a large population of approximately  $3 \times 10^4$  people opting for quarantine as a strategy. On the other hand, the burden for hospitals simultaneously shrinks, as anticipated, when a significant portion of the public participates in the decision-making process (Figure 9 (c)). Therefore, when  $p_s \leq 0.1$  and  $\eta_q \leq 0.293$  (Figure 9 (c)), a significant portion of the population is hospitalized, and concurrently,  $p_s$  has a greater influence on the payoff (Figure 9 (d)). Cumulative infected cases are extremely low ( $\approx 1 \times 10^5$ ) when  $\eta_q \leq 0.293$  and  $p_s \geq 0.495$  (Figure 9 (a)). In this case,  $1 - \eta_q$  will be extreme, so a huge proportion of the infected class shifts to the hospitalized compartment. Similarly, only a tiny percentage will eventually leave the quarantine area, but there will ultimately be a large cumulative population of quarantined individuals ( $\approx 2.5 \times 10^5$ ) (Figure 9 (b)).

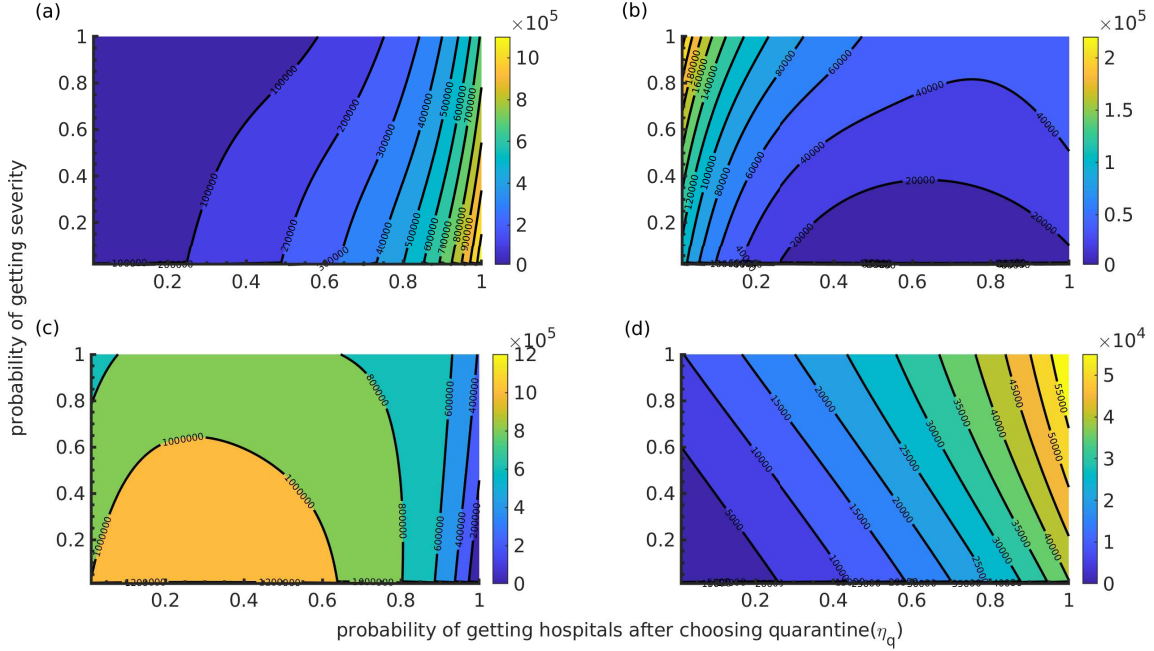


FIGURE 9. Figure represents the (a) cumulative infection (b) cumulative quarantined (c) cumulative hospitalized (d) cumulative new quarantined population per day; as a function of preference by public health authorities to provide treatment facility ( $\eta_q$ ) and probability of getting severity ( $p_s$ ), with  $c_d = 0.2$ ,  $c_{nd} = 0.2$ , and  $\kappa = 0.5$ .

We also analyzed the difference between the baseline payoff and the new payoff of the disclosure without  $1 - \eta_q$  to figure the importance of public health measures (Figure 9 & S2). We can see that cumulative hospitalization with our baseline payoff varies for greater values of  $\eta_q$  and  $p_s$  (Figure S2 (c)). When  $\eta_q$  is considered in our model, it mimics how public health interventions reduce the burden of disease, whether or not the condition is becoming severe. Based on our research, we hypothesize that the perceived severity of the illness is one of the main drivers of the increase in hospitalizations seen during the pandemic. If public health benefits are greater for the quarantined population, then a large proportion of the population will be involved in switching to disclose exposure. Understanding the true extent of the infection and effective public health messaging can motivate people to opt for quarantine.

**5.4. Data implementation, parameter estimation and scenario analysis.** We used historical hospitalized cases during COVID-19 from Chile, South America to estimate the parameters in our model (2.7). The total population of Chile was taken to be 19.6 million. We considered daily hospitalized cases during the period from April to September 2020. Since the model does not account for vaccination, We chose the time period of the data as the pre-vaccination period. The data set was acquired through the *Our World in Data* [50]. We estimate mostly FOI parameters and behavioural parameters (Table 3) denoted by  $\Theta_e$ :

$$\Theta_e = \{\beta_s, \beta_e, \eta_q, C_d, C_{nd}, \kappa, A, p_s, \zeta\}$$

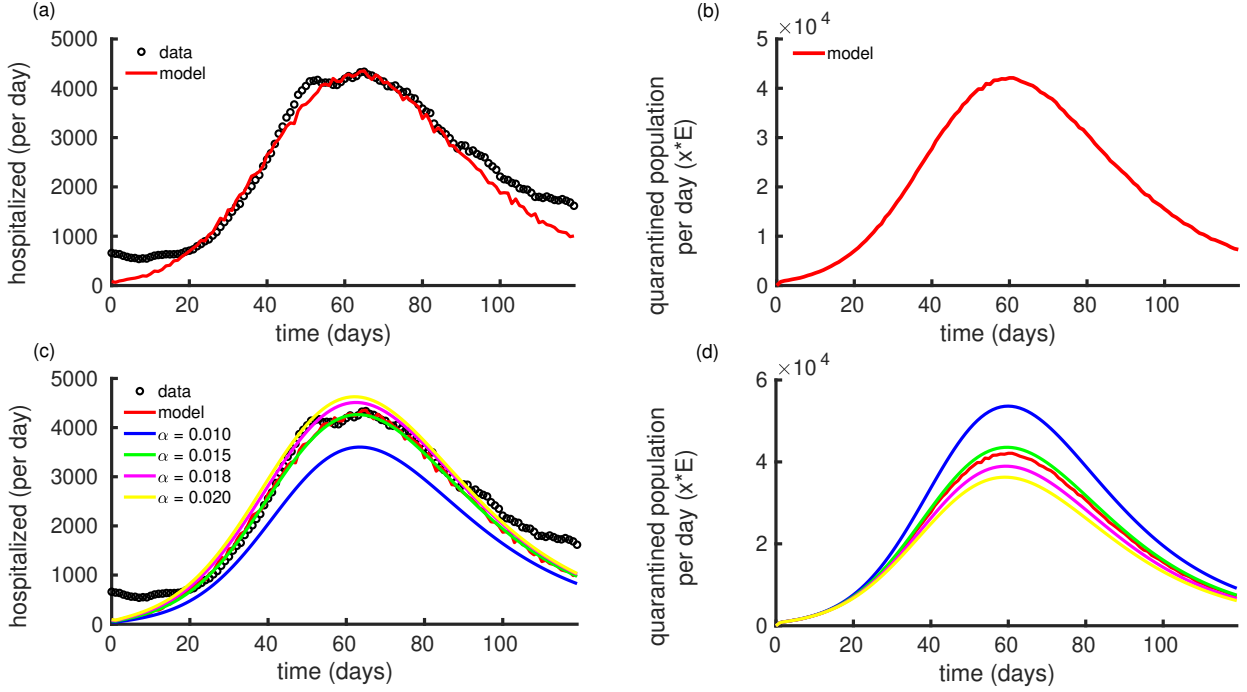


FIGURE 10. Figure represents the dynamics of (a) model fit to the confirmed new daily hospitalized in Chile, South America for the period from April to September, 2020; (b) quarantined population per day with estimated parameters. (c-d) plots of scenario analysis for different values of  $\alpha$ . For details, see the text.

Other parameters were kept fixed, obtained mostly from the literature (see Table 4). We used the Least square Approximation (LSA) approach to estimate the parameters. As depicted in Figure 10(a), our disclosure game model captures the pattern of hospitalized cases nicely, especially the peak timing and the duration of the outbreak. The goodness of fit ( $R^2$ ) is approximately 0.95037, indicating a relatively strong predictive power of our model, although the model can't reproduce the pattern in the data at the very beginning and the very end of the outbreak. This is most likely due to the fact that our model ignores comorbidity factors, which were common during COVID-19 hospitalization. According to some statistics, it was observed that 75% of hospitalized patients with COVID-19 have at least one comorbidity. The most common among these are hypertension, diabetes, cancer, neurodegenerative diseases, cardiovascular diseases, obesity, and kidney diseases [67]. The estimated parameter values are given in Table 3. Along with these parameters, we also estimate the initial condition:  $S(0) = 19623948.960$ ,  $E(0) = 0$ ,  $Q(0) = 0$ ,  $I(0) = 8592.1279$ ,  $H(0) = 11.509$ ,  $R(0) = 0$ ,  $x(0) = 0.35805$ . We also calculated the basic reproduction number  $R_0$  with estimated parameters, which turned out to be 2.6876. Since this value is greater than 1, it signifies an active force of infection, hence leading to increased hospitalizations, which is in agreement with our model-fitting result. The detailed method of estimation is given in the Supplementary Information (SI). We also plotted the daily disclosing population with the estimated parameters, which estimates around 45000 individuals possibly took part in disclosing their infection and being quarantined during

TABLE 3. Estimated parameter values in  $\Theta_e$ .

Parameters	Description	Optimized values (unit)
$\beta_s$	Mean disease transmission rate	0.262849 (per day)
$\beta_e$	Mean incubation rate	0.97278 (per day)
$\eta_q$	Preference by public health authorities to provide treatment facility	0.45296
$\zeta$	Order of fractional derivative	0.84552
$\kappa$	Sampling rate in social learning	0.016914 (per day)
$A$	Half saturation coefficient	545.976
$c_d$	Per unit cost of disclosing infection	0.09425
$c_{nd}$	Per unit cost of non-disclosing infection	1.5053
$p_s$	Probability of developing severity upon infection	0.918087

TABLE 4. Fixed parameter values

Parameters	Description	Values (per day)	ref.
$\alpha$	Rate of hospital admissions	0.016	[65]
$\gamma$	Recovery rate from infection	0.1	[15]
$\gamma_h$	Recovery rate of hospitalized patients	0.067	[68]
$\mu_h$	Mortality rate after hospitalization	0.011	[60]

the peak timing of the outbreak (Figure 10(b)). To have further examination, we tested the different scenarios of hospital admission rate ( $\alpha$ ) under the estimated parameters (Figure 10(c-d)). It changes the number of hospital admissions and the daily quarantine population.

## 6. DISCUSSION

The COVID-19 pandemic presented a multifaceted challenge to public health systems and communities worldwide [16, 71, 13]. Managing the spread of the SARS-CoV-2 virus necessitated a comprehensive approach, with individual actions playing a crucial role in the collective battle against the pandemic [24, 17]. Individual actions in the form of early detection and isolation have been consistently highlighted as a critical component of pandemic control [23, 30]. When individuals promptly recognize symptoms, get tested, and self-isolate upon a positive result, they prevent further spread of the virus within their communities [62, 69]. However, in most cases, the individual action was voluntary, i.e., public health authorities encourage individuals to disclose the infection and eventually quarantine if they are exposed to other infected people in the community, which turns out to be an individual decision-making initiative because this always incurs some cost. In our research, we have investigated how individual decision-making changes with several aspects of the transmission of infection in society or the availability of hospital beds in the community.

We investigated this decision-making approach by developing a standard SEIR (susceptible-exposed-infected-recovered) model, including hospital and quarantine compartments. We use a fractional derivative approach to represent disease propagation within a population.

We have shown that a rise in the rate of disease transmission leads to an increase in the illness burden and the load placed on hospitals. Consequently, an increased number of individuals will be involved in the decision-making process. The concomitant impact of public health interventions and disease transmission rates will decrease the population's hospitalization rate, although it increases with the severity of the disease. Taken together, our research highlights that quarantine may be a favorable strategy at the individual level in specific epidemiological situations. This may provide insights for public health officials in developing intervention plans to control an epidemic.

There are very recent works on game theory modeling in social isolation behaviour and its impact on disease control [34, 61]. Our paper takes a distinct approach from these referenced works, although there is significant overlap in motivations and applications. For instance, while Hossein et al. (2021 [41]) and Saad-Roy et al. (2023 [61]) presume that susceptible individuals are the players who can choose to adhere to Non-Pharmaceutical Interventions (NPIs), our model assumes that exposed individuals are the players in the game. Consequently, the availability of hospital beds drives behavioural choices in our model, unlike in the other cited research. For the same rationale, the fundamental disparity between our work and theirs lies in how we implement the control of infection transmission. Whereas our approach focuses on reducing infection within the community by decreasing the number of infected individuals, their methods primarily revolve around depleting susceptible individuals from the population to achieve the same goal. Additionally, unlike the referenced works that assume reinfection and demonstrate oscillating dynamics, we have excluded reinfection from our system.

Evolutionary game theory has now provided insightful perspectives on the evolution of behaviours during epidemics. Recently, it has applications in diverse emerging fields, encompassing complex networks, biological physics, and cyberphysical systems [76, 59, 31, 55, 53]. On the other hand, the fractional order technique has been used to model tumor growth, drug transport, immune response, and inflammation dynamics [25, 54, 5]. To compare the dynamical pattern generated by the fractional differential equation model with the ODE model, we conducted simulations across various fractional order values and compared them with traditional ordinary differential equation (ODE) simulations. Remarkably, as the fractional order ( $\zeta$ ) converges towards 1, ODE results exhibit convergence with fractional models (figure S3). We also found that the fractional-order derivative model fits the hospitalized data better than the ordinary differential equation (ODE) model (figure S4). Details are given in the Supplementary Information (SI).

While the current research has furnished a valuable framework for understanding the importance of quarantine as a strategy for controlling disease outbreaks, our model is based on simplified assumptions in many aspects. There are scopes for improvement in the analysis. The analysis can be broadened to examine how the periodicity of infection dynamics interacts with the fluctuation of individual choices. In our model, we have simplified the population as being uniform in age, not accounting for age-specific behaviours, which is very natural [75, 1]. To enhance the realism of the quarantine strategy, a heterogeneous population could be integrated [19]. From the perspective of epidemiological studies, it is also worthwhile to take into account the impact of disease severity on infection or even look into infection-disclosing behaviours during the vaccine's availability.

Nonetheless, our research provides a forum for discussion on individuals' perceptions of disclosing infection at the start of an epidemic. It also explores the causes and consequences of individuals' strategic decision-making in the face of different epidemiological conditions. Individuals always maximize their payoff while ignoring population-level externalities when making such decisions, but understanding the complex interaction is critical from a public health perspective because it may aid in disease outbreak management for the benefit of individual health in the community

#### CREDIT AUTHORSHIP CONTRIBUTION STATEMENT

**Pranav Verma:** Coding, Methodology, Formal analysis, Writing – original draft. **Viney Kumar:** Coding, Methodology, Formal analysis, Writing – original draft. **Samit Bhattacharyya:** Conceptualization, Methodology, Formal analysis, Writing – review & editing, Supervision.

#### DATA AVAILABILITY

The COVID-19 case data used in this manuscript is open-access data.

#### ACKNOWLEDGMENTS

The authors thank all reviewers for their insightful comments and suggestions for improving the presentation of the content in the manuscript. This work was initiated under the Shiv Nadar Institution of Eminence (SNIOE)'s Opportunity for Undergraduate Research (OUR) program. Viney Kumar thanks the Council of Scientific and Industrial Research (FILE NUMBER 09/1128(12030)/2021-EMR-I), India, for its financial support. All authors acknowledge SNIOE DST-FIST-funded computational lab support.

#### CONFLICT OF INTEREST

The authors declare that they have no known competing financial interests or personal relationships that could have appeared to influence the work reported in this paper.

#### REFERENCES

- [1] Emmanuel Addai, Lingling Zhang, Joshua KK Asamoah, and John Fiifi Essel. A fractional order age-specific smoke epidemic model. *Applied Mathematical Modelling*, 119:99–118, 2023.
- [2] Muntasir Alam and Jun Tanimoto. A game-theoretic modeling approach to comprehend the advantage of dynamic health interventions in limiting the transmission of multi-strain epidemics. *Journal of Applied Mathematics and Physics*, 10(12):3700–3748, 2022.
- [3] Amjad Ali, Muhammad Yasin Khan, Muhammad Sinan, FM Allehiany, Emad E Mahmoud, Abdel-Haleem Abdel-Aty, and Gohar Ali. Theoretical and numerical analysis of novel covid-19 via fractional order mathematical model. *Results in physics*, 20:103676, 2021.
- [4] Hussam Alrabaiah, Muhammad Arfan, Kamal Shah, Ibrahim Mahariq, and Aman Ullah. A comparative study of spreading of novel corona virus disease by using fractional order modified seir model. *Alexandria Engineering Journal*, 60(1):573–585, 2021.
- [5] David Ikechukwu Amilo, Khadijeh Sadri, Bilgen Kaymakamzade, and Evren Hincal. A mathematical model with fractional-order dynamics for the combined treatment of metastatic colorectal cancer. *Available at SSRN 4575187*, 2023.
- [6] Peter Ashcroft, Sonja Lehtinen, Daniel C Angst, Nicola Low, and Sebastian Bonhoeffer. Quantifying the impact of quarantine duration on covid-19 transmission. *Elife*, 10:e63704, 2021.
- [7] Dumitru Baleanu, Kai Diethelm, Enrico Scalas, and Juan J Trujillo. *Fractional calculus: models and numerical methods*, volume 3. World Scientific, 2012.

- [8] Chris T Bauch. Imitation dynamics predict vaccinating behaviour. *Proceedings of the Royal Society B: Biological Sciences*, 272(1573):1669–1675, 2005.
- [9] Chris T Bauch and Samit Bhattacharyya. Evolutionary game theory and social learning can determine how vaccine scares unfold. *PLoS computational biology*, 8(4):e1002452, 2012.
- [10] Samit Bhattacharyya and Chris T Bauch. “wait and see” vaccinating behaviour during a pandemic: a game theoretic analysis. *Vaccine*, 29(33):5519–5525, 2011.
- [11] Samit Bhattacharyya and CT Bauch. A game dynamic model for delayer strategies in vaccinating behaviour for pediatric infectious diseases. *Journal of theoretical biology*, 267(3):276–282, 2010.
- [12] Samit Bhattacharyya and Timothy Reluga. Game dynamic model of social distancing while cost of infection varies with epidemic burden. *IMA Journal of Applied Mathematics*, 84(1):23–43, 2019.
- [13] Alessandro Ceci, Carmen Munoz-Ballester, Allison N Tegge, Katherine L Brown, Robyn Anne Umans, F Marc Michel, Dipankumar Patel, Bhanu Tewari, Joelle Martin, Oscar Alcoreza, et al. Development and implementation of a scalable and versatile test for covid-19 diagnostics in rural communities. *Nature Communications*, 12(1):4400, 2021.
- [14] Muge Cevik, Stefan D Baral, Alex Crozier, and Jackie A Cassell. Support for self-isolation is critical in covid-19 response, 2021.
- [15] Seo Yoon Chae, KyoungEun Lee, Hyun Min Lee, Nam Jung, Quang Anh Le, Biseko Juma Mafwele, Tae Ho Lee, Doo Hwan Kim, and Jae Woo Lee. Estimation of infection rate and predictions of disease spreading based on initial individuals infected with covid-19. *Frontiers in Physics*, 8:311, 2020.
- [16] Carlo Contini, Elisabetta Caselli, Fernanda Martini, Martina Maritati, Elena Torreggiani, Silva Seraceni, Fortunato Vesce, Paolo Perri, Leonzio Rizzo, and Mauro Tognon. Covid-19 is a multifaceted challenging pandemic which needs urgent public health interventions. *Microorganisms*, 8(8):1228, 2020.
- [17] Alakesh Das, Surajit Pathak, Madhavi Premkumar, Chitra Veena Sarpparajan, Esther Raichel Balaji, Asim K Duttaroy, and Antara Banerjee. A brief overview of sars-cov-2 infection and its management strategies: a recent update. *Molecular and Cellular Biochemistry*, pages 1–21, 2023.
- [18] Angela Davis, Stephanie Munari, Joseph Doyle, Brett Sutton, Allen Cheng, Margaret Hellard, and Lisa Gibbs. Quarantine preparedness—the missing factor in covid-19 behaviour change? qualitative insights from australia. *BMC public health*, 22(1):1–10, 2022.
- [19] Fernando Díaz, Pablo A Henríquez, and Diego Winkelried. Heterogeneous responses in google trends measures of well-being to the covid-19 dynamic quarantines in chile. *Scientific Reports*, 12(1):14514, 2022.
- [20] Kai Diethelm, Neville J Ford, and Alan D Freed. A predictor-corrector approach for the numerical solution of fractional differential equations. *Nonlinear Dynamics*, 29:3–22, 2002.
- [21] Kai Diethelm and NJ Ford. The analysis of fractional differential equations. *Lect. Notes Math*, 2004:3–12, 2010.
- [22] Li Duan and Gang Zhu. Psychological interventions for people affected by the covid-19 epidemic. *The lancet psychiatry*, 7(4):300–302, 2020.
- [23] Anwesha Dutta and Harry W Fischer. The local governance of covid-19: Disease prevention and social security in rural india. *World Development*, 138:105234, 2021.
- [24] Aziz Eftekhari, Mahdieh Alipour, Leila Chodari, Solmaz Maleki Dizaj, Mohammadreza Ardalan, Mohammad Samiei, Simin Sharifi, Sepideh Zununi Vahed, Irada Huseynova, Rovshan Khalilov, et al. A comprehensive review of detection methods for sars-cov-2. *Microorganisms*, 9(2):232, 2021.
- [25] Muhammad Farman, Ali Akgül, Aqeel Ahmad, and Sumiyah Imtiaz. Analysis and dynamical behavior of fractional-order cancer model with vaccine strategy. *Mathematical Methods in the Applied Sciences*, 43(7):4871–4882, 2020.
- [26] Sebastian Funk, Marcel Salathé, and Vincent AA Jansen. Modelling the influence of human behaviour on the spread of infectious diseases: a review. *Journal of the Royal Society Interface*, 7(50):1247–1256, 2010.
- [27] Addis Adera Gebru, Tadesse Birhanu, Eshetu Wendimu, Agumas Fentahun Ayalew, Selamawit Mulat, Hussien Zakir Abasimel, Ali Kazemi, Bosenu Abera Tadesse, Beniam Adera Gebru, Berhanu Senbeta Deriba, et al. Global burden of covid-19: Situational analysis and review. *Human antibodies*, 29(2):139–148, 2021.

- [28] Aritra Ghosh, Srijita Nundy, and Tapas K Mallick. How india is dealing with covid-19 pandemic. *Sensors International*, 1:100021, 2020.
- [29] Christi A Grimm. Hospital experiences responding to the covid-19 pandemic: results of a national pulse survey march 23–27, 2020. *US Department of Health and Human Services Office of Inspector General*, 41:2020–04, 2020.
- [30] Hatice Rahmet Güner, İmran Hasanoglu, and Firdevs Aktaş. Covid-19: Prevention and control measures in community. *Turkish Journal of medical sciences*, 50(9):571–577, 2020.
- [31] Ashkan Hafezalkotob, Lia Nersesian, and Keyvan Fardi. A policy-making model for evolutionary sme behavior during a pandemic recession supported on game theory approach. *Computers & Industrial Engineering*, 177:108975, 2023.
- [32] Shaobo He, Yuexi Peng, and Kehui Sun. Seir modeling of the covid-19 and its dynamics. *Nonlinear dynamics*, 101:1667–1680, 2020.
- [33] Josef Hofbauer, Karl Sigmund, et al. *Evolutionary games and population dynamics*. Cambridge university press, 1998.
- [34] M Pear Hossain, Alvin Junus, Xiaolin Zhu, Pengfei Jia, Tzai-Hung Wen, Dirk Pfeiffer, and Hsiang-Yu Yuan. The effects of border control and quarantine measures on the spread of covid-19. *Epidemics*, 32:100397, 2020.
- [35] Yunhan Huang and Quanyan Zhu. Game-theoretic frameworks for epidemic spreading and human decision-making: A review. *Dynamic Games and Applications*, 12(1):7–48, 2022.
- [36] C Ionescu, A Lopes, Dana Copot, JA Tenreiro Machado, and Jason HT Bates. The role of fractional calculus in modeling biological phenomena: A review. *Communications in Nonlinear Science and Numerical Simulation*, 51:141–159, 2017.
- [37] Youngmee Jee. Who international health regulations emergency committee for the covid-19 outbreak. *Epidemiology and health*, 42, 2020.
- [38] Megha Kapoor, Karuna Nidhi Kaur, Shazina Saeed, Mohd Shannawaz, and Amrish Chandra. Impact of covid-19 on healthcare system in india: A systematic review. *Journal of Public Health Research*, 12(3):22799036231186349, 2023.
- [39] Simran Preet Kaur and Vandana Gupta. Covid-19 vaccine: A comprehensive status report. *Virus research*, 288:198114, 2020.
- [40] Alexander Keimer and Lukas Pflug. Modeling infectious diseases using integro-differential equations: Optimal control strategies for policy decisions and applications in covid-19. *Res Gate*, 10, 2020.
- [41] Hossein Khazaei, Keith Paarporn, Alfredo Garcia, and Ceyhun Eksin. Disease spread coupled with evolutionary social distancing dynamics can lead to growing oscillations. In *2021 60th IEEE Conference on Decision and Control (CDC)*, pages 4280–4286. IEEE, 2021.
- [42] Adem Kilicman et al. A fractional order sir epidemic model for dengue transmission. *Chaos, Solitons & Fractals*, 114:55–62, 2018.
- [43] Moritz UG Kraemer, Chia-Hung Yang, Bernardo Gutierrez, Chieh-Hsi Wu, Brennan Klein, David M Pigott, Open COVID-19 Data Working Group†, Louis Du Plessis, Nuno R Faria, Ruoran Li, et al. The effect of human mobility and control measures on the covid-19 epidemic in china. *Science*, 368(6490):493–497, 2020.
- [44] Laxmi, Calistus N Ngonghala, and Samit Bhattacharyya. An evolutionary game model of individual choices and bed net use: elucidating key aspect in malaria elimination strategies. *Royal Society Open Science*, 9(11):220685, 2022.
- [45] Ya-Ling Lee, Hsiao-Yun Hu, Yung-Feng Yen, Dachen Chu, Nan-Ping Yang, Sin-Yi Chou, Shu-Yi Lin, Chao-Mei Chu, and Sheng-Jean Huang. Impact of the covid-19 pandemic on the utilization of medical and dental services in taiwan: A cohort study. *Journal of dental sciences*, 16(4):1233–1240, 2021.
- [46] Lei Lei, Xiaoming Huang, Shuai Zhang, Jinrong Yang, Lin Yang, and Min Xu. Comparison of prevalence and associated factors of anxiety and depression among people affected by versus people unaffected by quarantine during the covid-19 epidemic in southwestern china. *Medical science monitor: international medical journal of experimental and clinical research*, 26:e924609–1, 2020.
- [47] Xiuli Liu, Geoffrey Hewings, Shouyang Wang, Minghui Qin, Xin Xiang, Shan Zheng, and Xuefeng Li. Modelling the situation of covid-19 and effects of different containment strategies in china with dynamic differential equations and parameters estimation. *medRxiv*, pages 2020–03, 2020.



- [48] Bhawna Malik, Habib Hasan Farooqui, and Samit Bhattacharyya. Disparity in socio-economic status explains the pattern of self-medication of antibiotics in india: understanding from game-theoretic perspective. *Royal Society open science*, 9(2):211872, 2022.
- [49] Maia Martcheva, Necibe Tuncer, and Calistus N Ngonghala. Effects of social-distancing on infectious disease dynamics: an evolutionary game theory and economic perspective. *Journal of Biological Dynamics*, 15(1):342–366, 2021.
- [50] Edouard Mathieu, Hannah Ritchie, Lucas Rodés-Guirao, Cameron Appel, Charlie Giatino, Joe Hasell, Bobbie Macdonald, Saloni Dattani, Diana Beltekian, Esteban Ortiz-Ospina, and Max Roser. Coronavirus pandemic (covid-19). *Our World in Data*, 2020. <https://ourworldindata.org/coronavirus>.
- [51] Faïçal Ndaïrou, Iván Area, Juan J Nieto, and Delfim FM Torres. Mathematical modeling of covid-19 transmission dynamics with a case study of wuhan. *Chaos, Solitons & Fractals*, 135:109846, 2020.
- [52] Ruiwu Niu, Eric WM Wong, Yin-Chi Chan, Michaël Antonie Van Wyk, and Guanrong Chen. Modeling the covid-19 pandemic using an seihmr model with human migration. *Ieee Access*, 8:195503–195514, 2020.
- [53] Magdalena Ochab, Piero Manfredi, Krzysztof Puzynski, and Alberto d’Onofrio. Multiple epidemic waves as the outcome of stochastic sir epidemics with behavioral responses: a hybrid modeling approach. *Nonlinear Dynamics*, 111(1):887–926, 2023.
- [54] Nikhil Pachauri, Velamuri Suresh, MVV Prasad Kantipudi, Reem Alkanhel, and Hanaa A Abdallah. Multi-drug scheduling for chemotherapy using fractional order internal model controller. *Mathematics*, 11(8):1779, 2023.
- [55] Gamaliel A Palomo-Briones, Mario Siller, and Arnaud Grignard. An agent-based model of the dual causality between individual and collective behaviors in an epidemic. *Computers in biology and medicine*, 141:104995, 2022.
- [56] Claire Pentecost, Rachel Collins, Sally Stapley, Christina Victor, Catherine Quinn, Alexandra Hillman, Rachael Litherland, Louise Allan, and Linda Clare. Effects of social restrictions on people with dementia and carers during the pre-vaccine phase of the covid-19 pandemic: Experiences of ideal cohort participants. *Health & social care in the community*, 30(6):e4594–e4604, 2022.
- [57] Prashant Premkumar, Jimut Bahan Chakrabarty, and A Rajeev. Impact of sustained lockdown during covid-19 pandemic on behavioural dynamics through evolutionary game theoretic model. *Annals of Operations Research*, pages 1–17, 2023.
- [58] Fathalla A Rihan. Dynamics of salmonella infection. *Book Chapter in” Current Topics in Salmonella and Salmonellosis”(Editor: Mihai Mares*, pages 151–167, 2017.
- [59] Amal Roy, Chandramani Singh, and Y Narahari. Recent advances in modeling and control of epidemics using a mean field approach. *Sādhanā*, 48(4):207, 2023.
- [60] Piotr Rzymiski, Nadiia Kasianchuk, Dominika Sikora, and Barbara Poniedziałek. Covid-19 vaccinations and rates of infections, hospitalizations, icu admissions, and deaths in europe during sars-cov-2 omicron wave in the first quarter of 2022. *Journal of Medical Virology*, 95(1):e28131, 2023.
- [61] Chadi M Saad-Roy and Arne Traulsen. Dynamics in a behavioral–epidemiological model for individual adherence to a nonpharmaceutical intervention. *Proceedings of the National Academy of Sciences*, 120(44):e2311584120, 2023.
- [62] Marcel Salathé, Christian L Althaus, Richard Neher, Silvia Stringhini, Emma Hodcroft, Jacques Fellay, Marcel Zwahlen, Gabriela Senti, Manuel Battegay, Annelies Wilder-Smith, et al. Covid-19 epidemic in switzerland: on the importance of testing, contact tracing and isolation. *Swiss medical weekly*, 150(1112):w20225–w20225, 2020.
- [63] Abhisek Satapathi, Narendra Kumar Dhar, Ashish R Hota, and Vaibhav Srivastava. Coupled evolutionary behavioral and disease dynamics under reinfection risk. *IEEE Transactions on Control of Network Systems*, 2023.
- [64] Ashley A Schiffer, Conor J O’Dea, and Donald A Saucier. Moral decision-making and support for safety procedures amid the covid-19 pandemic. *Personality and Individual Differences*, 175:110714, 2021.
- [65] Brendon Sen-Crowe, Mason Sutherland, Mark McKenney, and Adel Elkbuli. A closer look into global hospital beds capacity and resource shortages during the covid-19 pandemic. *Journal of Surgical Research*, 260:56–63, 2021.

- [66] Kamal Shah, Amjad Ali, Salman Zeb, Aziz Khan, Manar A Alqudah, and Thabet Abdeljawad. Study of fractional order dynamics of nonlinear mathematical model. *Alexandria Engineering Journal*, 61(12):11211–11224, 2022.
- [67] Radu Silaghi-Dumitrescu, Iulia Patrascu, Maria Lehene, and Iulia Bercea. Comorbidities of covid-19 patients. *Medicina*, 59(8):1393, 2023.
- [68] Haoxuan Sun, Yumou Qiu, Han Yan, Yaxuan Huang, Yuru Zhu, Jia Gu, and Song Xi Chen. Tracking reproductivity of covid-19 epidemic in china with varying coefficient sir model. *Journal of Data Science*, 18(3):455–472, 2020.
- [69] Rachael J Thorneloe, Elaine N Clarke, and Madelynne A Arden. Adherence to behaviours associated with the test, trace, and isolate system: an analysis using the theoretical domains framework. *BMC Public Health*, 22(1):1–11, 2022.
- [70] Bharath Kumar Tirupakuzhi Vijayaraghavan, Sheila Nainan Myatra, Meghena Mathew, Nirmalyo Lodh, Jigeeshu Vasishtha Divatia, Naomi Hammond, Vivekanand Jha, and Balasubramanian Venkatesh. Challenges in the delivery of critical care in india during the covid-19 pandemic. *Journal of the Intensive Care Society*, 22(4):342–348, 2021.
- [71] Muhammad Nawaz Tunio, Erum Shaikh, Sheeraz Lighari, et al. Multifaceted perils of the covid-19 and implications: A review. *Studies of Applied Economics*, 39(2), 2021.
- [72] Mohammad Sharif Ullah, M Higazy, and KM Ariful Kabir. Dynamic analysis of mean-field and fractional-order epidemic vaccination strategies by evolutionary game approach. *Chaos, Solitons & Fractals*, 162:112431, 2022.
- [73] Mubashara Wali, Sadia Arshad, and Jianfei Huang. Stability analysis of an extended seir covid-19 fractional model with vaccination efficiency. *Computational & Mathematical Methods in Medicine*, 2022.
- [74] Xianliang Wang, Jiao Wang, Jin Shen, John S Ji, Lijun Pan, Hang Liu, Kangfeng Zhao, Li Li, Bo Ying, Lin Fan, et al. Facilities for centralized isolation and quarantine for the observation and treatment of patients with covid-19. *Engineering*, 7(7):908–913, 2021.
- [75] George Wittemyer, David Daballen, and Iain Douglas-Hamilton. Differential influence of human impacts on age-specific demography underpins trends in an african elephant population. *Ecosphere*, 12(8):e03720, 2021.
- [76] Bingjing Yan, Zhenze Jiang, Pengchao Yao, Qiang Yang, Wei Li, and Albert Y Zomaya. Game theory based optimal defensive resources allocation with incomplete information in cyber-physical power systems against false data injection attacks. *Protection and Control of Modern Power Systems*, 9(2):115–127, 2024.
- [77] Bo Yang, Zhenhua Yu, and Yuanli Cai. A spread model of covid-19 with some strict anti-epidemic measures. *Nonlinear Dynamics*, 109(1):265–284, 2022.
- [78] Akeem O Yunus, Morufu O Olayiwola, Kamilu A Adedokun, Joseph A Adedeji, and Ismaila A Alaje. Mathematical analysis of fractional-order caputo’s derivative of coronavirus disease model via laplace adomian decomposition method. *Beni-Suef University Journal of Basic and Applied Sciences*, 11(1):144, 2022.
- [79] Nataliia Zachosova, Dmytro Kutsenko, Oleksii Koval, and Andrii Kovalenko. Management of financial and economic security of critical infrastructure objects in the conditions of risks of quarantine restrictions: strategic and personnel aspects. In *SHS Web of Conferences*, volume 107, page 02002. EDP Sciences, 2021.
- [80] Anwar Zeb, Madad Khan, Gul Zaman, Shaher Momani, and Vedat Suat Ertürk. Comparison of numerical methods of the seir epidemic model of fractional order. *Zeitschrift für Naturforschung A*, 69(1-2):81–89, 2014.
- [81] Zhibao Zheng, Wei Zhao, and Hongzhe Dai. A new definition of fractional derivative. *International Journal of Non-Linear Mechanics*, 108:1–6, 2019.
- [82] Wenlong Zhu, Mengxi Zhang, Jinhua Pan, Ye Yao, and Weibing Wang. Effects of prolonged incubation period and centralized quarantine on the covid-19 outbreak in shijiazhuang, china: a modeling study. *BMC medicine*, 19:1–11, 2021.

PV: STUDENT, DEPARTMENT OF MATHEMATICS, SHIV NADAR UNIVERSITY, DELHI - NCR 201314, INDIA

*Email address:* `pv638@snu.edu.in`

VK: RESEARCH SCHOLAR, DEPARTMENT OF MATHEMATICS, SHIV NADAR UNIVERSITY, DELHI - NCR 201314, INDIA

*Email address:* `vk981@snu.edu.in`

SB: PROFESSOR, DEPARTMENT OF MATHEMATICS, SHIV NADAR UNIVERSITY, DELHI - NCR 201314, INDIA

*Email address:* `samit.b@snu.edu.in`